American Journal of Mechanics and Applications
2025, Vol. 12, No. 2, pp. 22-32
https://doi.org/10.11648/j.ajma.20251202.11

Research Article

A Numerical Implementation of Linear Matching Method for the Limit Analysis

Jun-Hyok Ri[1, *], Hyon-Sik Hong[1], Yong-Chol Kim[2], Jin-Chol Ri[2]

[1]Institute of Mechanics, State Academy of Sciences, Pyongyang, DPR Korea

[2]Department of Coal Mining Construction Engineering, Pyongsong University of Coal Mining, Pyongsong, DPR Korea

Abstract

ANSYS UserMat and its corresponding special MACRO are developed for implementing the linear matching method (LMM) for the limit analysis by using ANSYS. By this, pre and post-processing for the limit analysis can be done in the sole ANSYS circumstance without a help of any additional programs. Once user creates the FE model and enters the parameters for the LMM analysis by using ANSYS interface, ANSYS then will evaluate the upper and lower bound of limit load automatically. In order to overcome the drawback of LMM which does not give the reliable lower bound of limit load, the elastic compensation method (ECM) for the computation of lower bound of limit load is combined with the LMM so that the converged upper and lower bound of limit load is obtained, respectively. Moreover, a simple method is proposed in order to overcome the numerical difficulty of LMM due to the high gradient of stress state. Some numerical examples were given to validate the proposed method and the corresponding computational system and the reliable stability was shown, as expected.

Keywords

LMM, Limit Analysis, ANSYS UPF

1. Introduction

There have been developed various numerical approaches for the limit analysis of structures which could be classified as the direct method and the indirect one according to the solution category of optimization problems. The direct method usually consists of the linear elastic FEA, the computation of bases of residual stress field and the optimization, classifying into several methods according to the numerical method employed for the optimization [1, 2]. The indirect method, of which the LMM is a representative, is the one for obtaining the solution of limit load by the iterative computation of FEAs having special properties unlike the optimization method [3-5].

The convergence of LMM has already been proved and found wide applications for practice, leading to the confirmation of its accuracy [6, 7]. In particular, the LMM was applied for the determination of limit load of composites [8-11] and pressure vessels [19-23].

It is one of the greatest advantages of LMM that the standard FEA can be used, considering the varying spatially material properties, leading to the easy implementation by using the multi-purpose FEA packages like ANSYS, ABAQUS and ADINA. ABAQUS and ADINA has already

*Corresponding author: junhyok.ri.mech@star-co.net.kp (Jun-Hyok Ri)

Received: 26 February 2025; **Accepted:** 3 April 2025; **Published:** 9 May 2025

Copyright: © The Author(s), 2025. Published by Science Publishing Group. This is an **Open Access** article, distributed under the terms of the Creative Commons Attribution 4.0 License (http://creativecommons.org/licenses/by/4.0/), which permits unrestricted use, distribution and reproduction in any medium, provided the original work is properly cited.

been used for the limit analysis of structures based on the LMM, respectively [6, 9, 10, 12].

In this paper, ANSYS is implemented for the limit analysis of structure based on the LMM. Considering the varying spatially material properties, ANSYS UserMat and special MACRO for the pre and post-processing aimed to compute the upper and lower bound of limit load are developed and their implementation procedure is established. In order to overcome the drawback of LMM which does not give the reliable lower bound of limit load, the elastic compensation method (ECM) for the computation of the lower bound of limit load is combined with the LMM so that the converged upper and lower bound of limit load is obtained, respectively. Moreover, a simple method is proposed in order to overcome the numerical difficulty of LMM due to the high gradient of stress state. The computation system for the limit analysis is made so as to use the standard functions of ANSYS, reduce the amount of data processing and modify the code easily as possible as one can. Only if user creates the FE model by using ANSYS interface and executes the pre and post-processing MACRO, the upper and lower bound of limit load can be obtained automatically and viewed in the type of graph or list. This system can solve the plane stress, the plane strain and the axi-symmetry as well as the 3D problems using 3D SOLID and 2D SOLID elements.

Some numerical examples including the square plate with a circular hole, the single edge notched plate, axi-symmetric pressure vessel and the 3D pipe connection are shown in order to validate the proposed method and its corresponding execution system. The obtained results show the good agreement with the analytical ones as well as the excellent convergence.

2. Linear Matching Method for the Limit Analysis

2.1. Lower and Upper Bound Theorem of the Limit Load

Material is assumed to be elastic-perfectly-plastic and that satisfies the von Mises yielding condition. Let us consider a body with volume V and surface S where a traction is given as zero or $P \cdot p_i(x_i)$ on S_T and displacement $\bar{u}_i = 0$ is specified on S_u ($S = S_F + S_u$). Here, P is a scalar parameter defining the relative magnitude of applied load as compared with the reference load p_i. The lower and upper bound theorem of the limit load can be postulated as follows, respectively [5].

Lower bound theorem:

If, for load $P = P_{LB}$, there exists a statically possible stress field such that:

$$f\left(\sigma_{ij}^{*}\right) \le \sigma_y \tag{1}$$

at every point within V, then $P_L \ge P_{LB}$. Here, f is a von Mises yield function and σ_y is the uniaxial yield stress. Thus, one can know that the maximum value of P_{LB} is the lower bound of limit load.

Upper bound theorem:

If, for load $P = P_{UB}$, there exists a kinetically possible displacement rate field $\dot{u}_i^{*}$ and its corresponding strain rate field such that:

$$P_{UB} \int_{S_T} p_i \dot{u}_i^{*} = \int_V \sigma_{ij}^{p^*} \dot{\varepsilon} \dot{u}_{ij}^{*} dV \tag{2}$$

where $\sigma_{ij}^{p^*}$ is the stress point at yield associated with $\dot{\varepsilon}_{ij}^{*}$, then satisfies $P_L \le P_{UB}$. Hence, one can know that the minimum value of P_{UB} is the upper bound of limit load.

According to above theorems, lower and upper bound of the limit load could be evaluated by solving the optimization problem. The direct method employs the optimization approach based on the admissible space as the statically possible stress filed or the kinetically possible strain field, while the indirect method obtains the statically possible stress filed or the kinetically possible strain field by using FEA with a certain particular property, leading to the improvement of solution of the limit load. The LMM takes the kinetically possible strain field by the FEA solution obtained adjusting spatially varying material properties.

2.2. LMM Algorithm for the Limit Analysis

As mentioned above, the LMM is based on the linear elastic FEA with the spatially varying material properties. The Young's modulus is changed spatially such that stress field corresponding to a certain kinetically possible strain field is placed on the yielding surface at every point of material. The Poisson ratio is taken as 0.4999999 since the material has the plastic incompressibility. The LMM algorithm could be formulated as follows [3-5, 8].

1) Initialization: Set $P_{UB}^{0} = 1$, $E^{1}(\mathrm{x}) = E$.

2) k th iteration:

The linear elastic analysis with the Young's modulus of $E^{k}(\mathrm{x})$ is performed under a load $P_{UB}^{k-1} \cdot p$ and σ_{ij}^{k}, ε_{ij}^{k} and u_i^{k} is obtained, respectively.

Lower and upper bound of the limit load at k th iteration is evaluated as:

$$P_{LB}^{k} = P_{UB}^{k-1} \frac{\sigma_y}{\sigma_{eq}\left(\sigma_{ij}^{k}\right)} \tag{3}$$

$$P_{UB}^{k} = P_{UB}^{k-1} \frac{\int_V \sigma_y \varepsilon_{eq}\left(\varepsilon_{ij}^{k}\right)}{\int_{S_T} P_{UB}^{k-1} p_i u_i^k} \tag{4}$$

where, σ_{eq} and ε_{eq} denotes the equivalent stress and strain, respectively.

The E^{k+1} at $k+1$th iteration is updated as follows.

$$E^{k+1} = \frac{\sigma_y}{\varepsilon_{eq}\left(\varepsilon_{ij}^{k}\right)} \tag{5}$$

Equation (5) gives the E^{k+1} at $k+1$th iteration such that the stress field corresponding to the strain field ε_{ij}^{k} obtained at kth iteration lies on the yielding surface. Nevertheless, for the high gradient of stress, the Young's modulus evaluated by equation (5) may not give incorrect solution, sometimes. In order to overcome this numerical difficulty without any effect on the LMM solution, we do the normalization using the initial Young's modulus E_{ref} of material.

We denote the minimum value of the Young's modulus $E^{k}(\mathrm{x})$ on the whole region obtained at $k-1$th iteration by $E_{\min}^{k} = \min_{\mathrm{x}} E^{k}(\mathrm{x})$. Then, after performing the kth iteration, E^{k+1} at $k+1$th iteration will be evaluated by:

$$E^{k+1} = \frac{E_{ref}}{E_{\min}^{k}} \frac{\sigma_y}{\varepsilon_{eq}\left(\varepsilon_{ij}^{k}\right)} \tag{6}$$

instead of using equation (5). Even though equation (6) shows the theoretical equivalence with equation (5), our computational experiences ensure that equation (6) can improve the numerical stability much more as compared with equation (5).

Meanwhile, instead of using equation (5), the elastic compensation method (ECM) employs following relation [9].

$$E^{k+1} = \begin{cases} E & \sigma_{\mathrm{eq}}\left(\sigma_{ij}^{k}\right) < \sigma_y \\ \dfrac{\sigma_y}{\varepsilon_{eq}\left(\varepsilon_{ij}^{k}\right)} & \sigma_{\mathrm{eq}}\left(\sigma_{ij}^{k}\right) \geq \sigma_y \end{cases} \tag{7}$$

The LMM gives the non-increasing series of upper bound but fails to give the non-decreasing ones of lower bound, sometimes whereas the ECM results the non-increasing series of upper bound as well as the non-decreasing ones of lower bound even though the convergence rate of series of upper bound can not be rapid as compared with in the LMM.

Though the ECM has been emerged earlier in fact, it is used as the additional method for the theoretically completed LMM now. Moreover, the difference between two methods lies only in using equation (6) or equation (7), thus we don't distinguish the execution of LMM and ECM.

3. Implementaion of the LMM by Using ANSYS

ANSYS UserMat and pre and post-processing MACRO can be executed for the implementation of LMM. First, by compiling and connecting ANSYS UserMat, ANSYS.exe with adding the user-defined material is generated. And then the path of newly generated ANSYS.exe is added into Custom ANSYS Executable of Mechanical APDL Launcher. Finally ANSYS is executed.

In the meantime, pre and post-processing MACRO file is copied into the working directory. Next, after executing the pre-processing MACRO, parameters for the LMM is entered and FE model for the limit analysis is made. User can make the FE model by using GUI or ANSYS commands without the definition of material properties. It should be noted that the element integration formula appropriate for the non-compressible condition has to be used because the material follows nearly non-compressible property.

After the definition of FE model, the limit analysis using the LMM is performed automatically by executing the post-processing MACRO. According to the iteration number entered in the pre-processing MACRO, the LMM and the ECM is repeated.

3.1. ANSYS Subroutine-Usermat

It is impossible to compute the varying spatially Young's modulus evaluated by equation (5) or equation (6) by using the default functions of ANSYS. UserMat, being the ANSYS UPF subroutine, can be used in order to evaluate the varying spatially Young's modulus. UserMat controls such that the upper and lower bound of limit load evaluated according to equation (3) or equation (4) as well as the Young's modulus to be used in the next iteration can be output by the state variable of user-defined material or reflected in the default output of element. By this, it is possible to control the solution process sufficiently by using only the standard functions of ANSYS without any development of other programs for the post-processing of LMM or the additional treatment process. In other words, one has no need for making program or user subroutine in order to evaluate the upper and lower bound of limit load by reading the computed results from files.

3.2. Pre-Processing Macro

Figure 1 shows the execution of pre-processing MACRO. The pre-processing MACRO offers the ANSYS interface for the input of parameters necessary for the limit analysis based on the LMM and declares the associated variables.

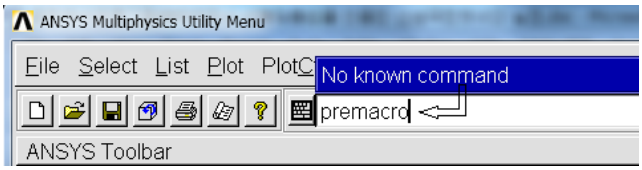

Figure 1. *Execution of pre-processing MACRO.*

Figure 2 presents the ANSYS interface for the input of parameters including the Young's modulus, the yield stress and the maximum iteration number of LMM. The reference solution is entered for the comparison if it would be known beforehand. If the reference solution is unknown or user does not want to view the comparison, this option should be entered by any value less than zero.

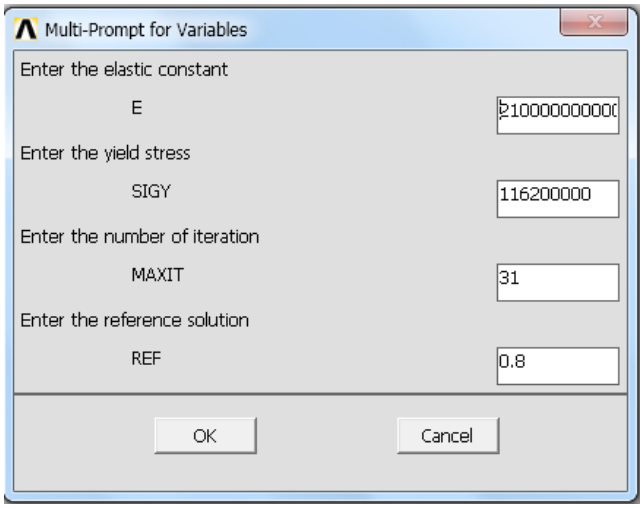

Figure 2. *ANSYS interface for the input of parameters.*

3.3. Post-Processing Macro

The post-processing MACRO performs the iteration computation by the maximum iteration number entered in the pre-processing MACRO according to the algorithm of LMM or ECM in order to evaluate the upper and lower bound of limit load. Furthermore, it displays the upper bound of limit loads calculated by the LMM as well as the lower one of limit load evaluated by the ECM using the graph. Meanwhile, the obtained solution is listed by the message. Figure 3 shows its example.

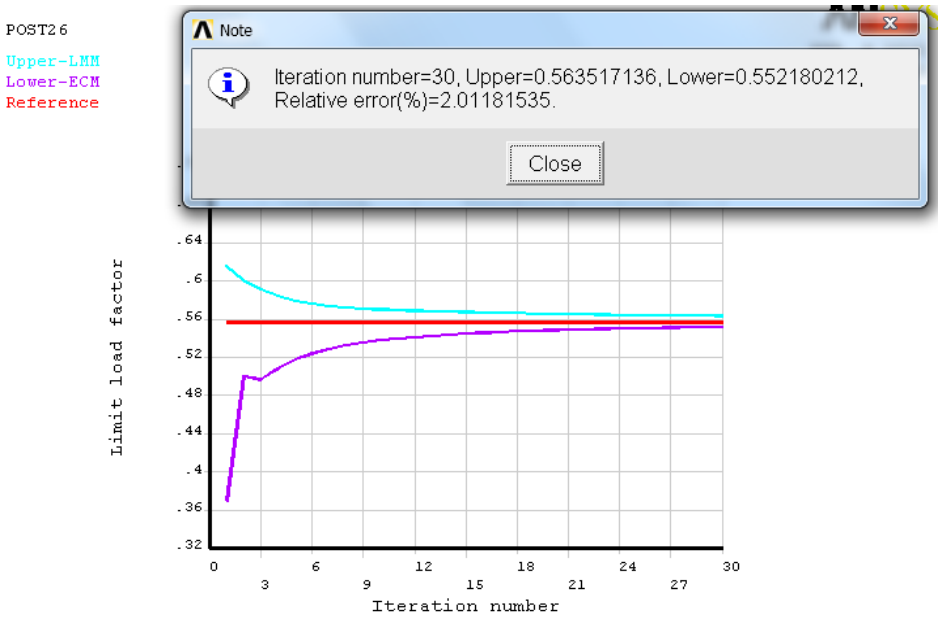

Figure 3. *Display and list in the form of graph and message by using the post-processing MACRO.*

4. Numerical Examples

4.1. The Square Plate with a Circular Hole

Figure 4 shows the FE model of square plate with a circular central hole under the biaxial tension. For the biaxial tension of $p_1 = p_2 = \sigma_y$, the analytical solution for the plane stress condition has already been known in ref [13].

Figure 5 depicts the upper and lower bound of limit load calculated by the LMM and the ECM, respectively.

Table 1 lists the numerical results for the upper and lower bound of limit load as compared with the analytical ones for different ratios of R/L, confirming the good agreement between them.

Table 1. *Analytical solutions as well as numerical ones for different ratios of* R/L.

R/L	Analytical solution	Upper bound for LMM	Lower bound for ECM
0.1	0.97063	0.97494	0.96341
0.2	0.89425	0.89987	0.87998
0.3	0.79122	0.79734	0.77751
0.4	0.67602	0.68274	0.66685
0.5	0.55682	0.56352	0.55128
0.6	0.43801	0.44441	0.43419
0.7	0.32195	0.32696	0.31511
0.8	0.20991	0.21257	0.20394
0.9	0.10249	0.10402	0.09977

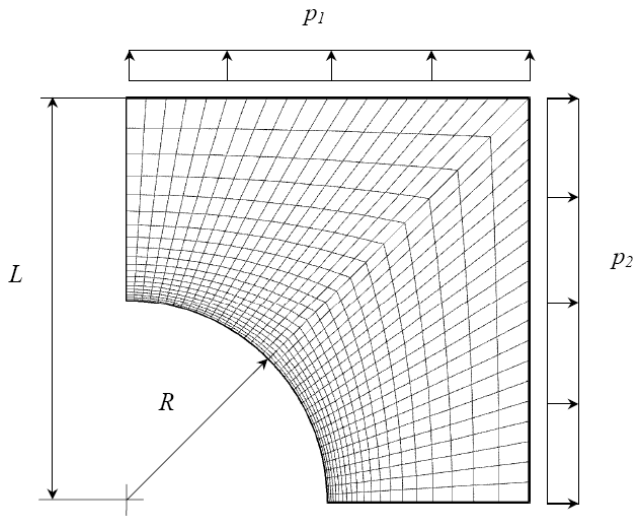

Figure 4. *Plate with a circular hole under the biaxial tension.*

As expected, one can see from Figure 5 that the LMM predicts the more accurate upper bound while the ECM evaluates the lower bound with the better accuracy, as mentioned above.

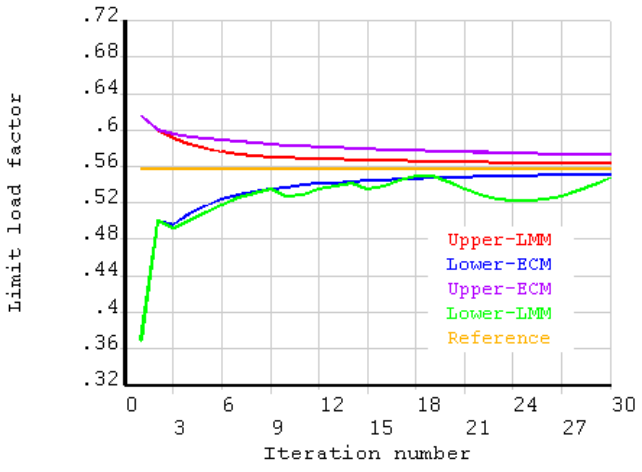

Figure 5. *Upper and lower bound of limit load computed by the LMM and the ECM for* $R/L = 0.5$.

After this, we obtain the upper bound by using the LMM and the lower one by the ECM.

4.2. The Single Edge Notched Plate Under Tension

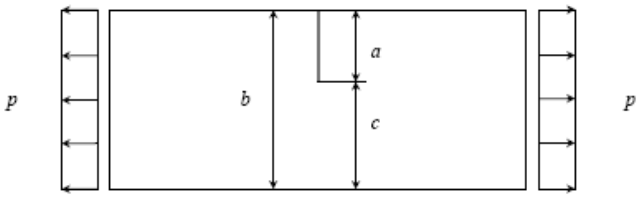

Figure 6. *Geometry of single edge notched plate under the tension.*

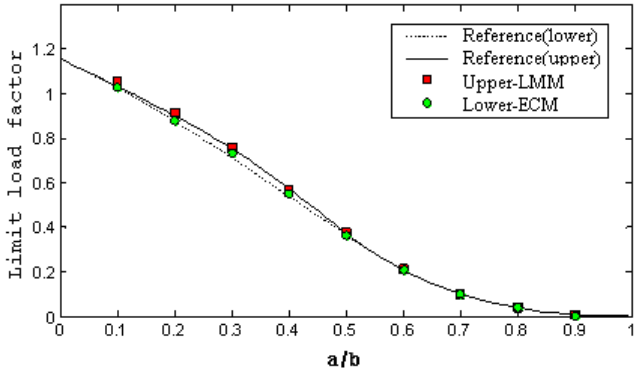

Figure 7. *Numerical result as well as analytical one [14, 15] for the single edge notched plate with different relative crack lengths.*

Figure 6 shows the geometry of single edge notched plate under the tension. Assuming the plane strain condition, the geometry of $b = L$ and the loading condition of $p = \sigma_y$ is applied, respectively.

Figure 7 presents the numerical result as well as the analytical one [14, 15] for the single edge notched plate with different relative crack lengths for the comparison.

As seen from this figure, our result has a good agreement with the analytical one.

4.3. Axi-Symmetric Pressure Vessel Subjected to the Internal Pressure

The axi-symmetric pressure vessel is studied, which has been investigated by many researchers, as shown in figure 8. The geometry of $R_b = 4500mm$, $R_z = L = 3000mm$, $l = 658.2mm$, $R_k = 360mm$ and $s = 225mm$ are assumed.

For the internal pressure of $p = \sigma_y$, the limit load factor is found as 0.0746~0.083 in ref [16] and as 0.78 in ref [17]. Through 40 iterations, the limit load factor of upper and lower bound was obtained as 0.785 and 0.772, respectively, which showed the good agreement with the result as in previously studies.

Figure 9 depicts the convergence process of upper and lower bound of limit load factor. As shown, one can know that the lower bound has a slow convergence rate as compared with the upper one.

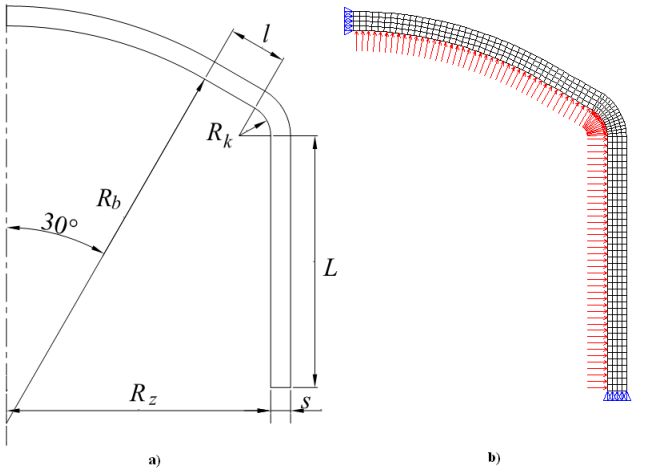

Figure 8. *Axi-symmetric pressure vessel: a) Geometry; b) FE model.*

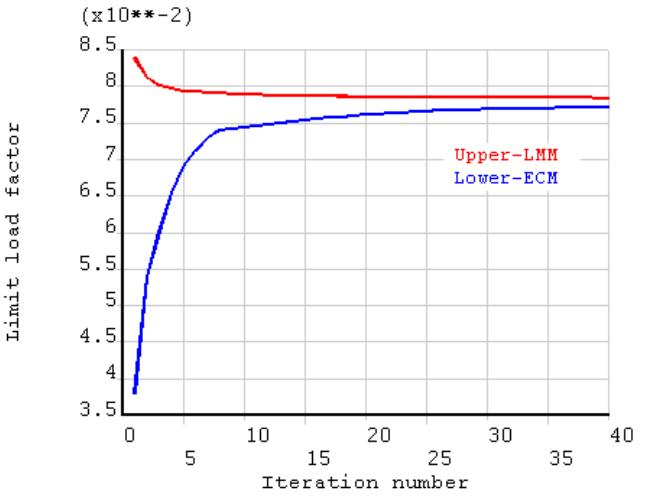

Figure 9. *Convergence process of the limit load factor of pressure vessel subjected to the internal pressure.*

4.4. The 3D Pipe Connection

The 3D pipe connection subjected to the internal pressure is considered for the limit analysis as shown in figure 10. The geometry of $D = 39mm$, $d = 15mm$ and $s = t = 3.4mm$ are assumed. For the internal pressure of $p = \sigma_y$, the limit load factor is known as 0.1443 in ref [17] and as 0.134 in ref [18].

Until 30 iterations, the upper and lower bound was obtained as 0.141 and 0.139, respectively, which confirmed the very good agreement with the previous results. Figure 11 shows the convergence process of solutions. As seen from this figure, the lower bound requires the more iteration number than the upper one to obtain the converged solutions.

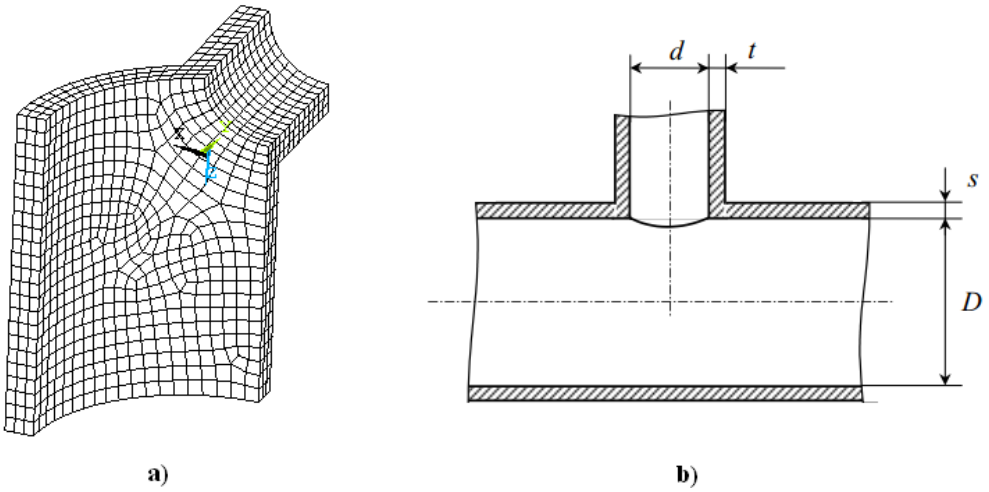

Figure 10. *3D pipe connection: a) FE mesh; b) Geometry.*

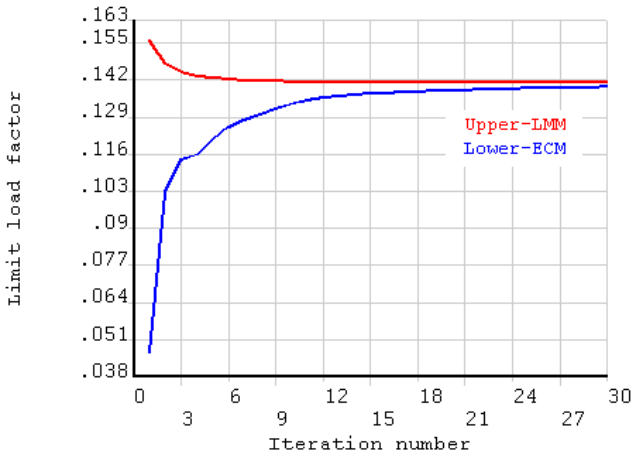

Figure 11. *Convergence process of limit load factor of pipe connection.*

5. Conclusions

In this paper, we developed the ANSYS user subroutines and the specific pre and post-processing MACROs for the limit analysis of structures and established its execution procedure by using ANSYS and LMM. And a simple method was proposed in order to raise the numerical stability of LMM. Our numerical results showed the good agreement with the previous one as well as high numerical stability.

This study is limited to the limit analysis for the monotonic external loading. In the future, the shakedown analysis for the general case when the variable loads act should be developed by using ANSYS, including the shell and the beam problem.

One can refer the ANSYS UserMat and some of pre and post-processing MACROs in appendix.

Abbreviations

LMM	Linear Matching Method
FE	Finite Element
ECM	Elastic Compensation Method
UPF	User Programmable Function

Conflicts of Interest

The authors declare no conflicts of interest.

Appendix

Appendix I: Usermat (Plane Stress)

```
*deck,usermatps      USERDISTRIB   parallel                                  gal
subroutine usermatps(
&                     matId, elemId,kDomIntPt, kLayer, kSectPt,
&                     ldstep,isubst,keycut,
&                     nDirect,nShear,ncomp,nStatev,nProp,
&                     Time,dTime,Temp,dTemp,
&                     stress,ustatev,dsdePl,sedEl,sedPl,epseq,
```

```
&                       Strain,dStrain, epsPl, prop, coords,
&                       var0, defGrad_t, defGrad,
&                       tsstif, epsZZ,
&                       var1, var2, var3, var4, var5,
&                       var6, var7, var8)

#include "impcom.inc"
INTEGER
&                       matId, elemId,
&                       kDomIntPt, kLayer, kSectPt,
&                       ldstep,isubst,keycut,
&                   nDirect,nShear,ncomp,nStatev,nProp
DOUBLE PRECISION
&                       Time,     dTime,     Temp,     dTemp,
&                       sedEl,    sedPl,     epseq,    epsZZ
c
c**********************************************************************
c
keycut    = 0
c ***     get young's modulus from array parameter 'YOUNG' and etc
young           = ustatev(1)
young_ref     = prop(1)
posn            = prop(2)
sigy0           = prop(3)
c
c *** calculate elastic stiffness matrix (2d)
c
c1 = ONE - posn * posn
c2 = young / c1
c3 = posn * c2
twoG        = young / (ONE+posn)
tsstif(1) = HALF * twoG
c *** identify LMM or ECM scheme
parName = 'LMM'
CALL PAREVL (parName, 0, 1, -1, LMM, cLabels, keyiqr)
parName = 'YOUNG_MIN'
CALL PAREVL (parName, 0, 1, -1, young_min, cLabels, keyiqr)
```

Appendix II: Pre-Processing Macro

```
PARSAV,SCALAR,'PARAM',' ',' '
PARRES,NEW,'PARAM',' ',' '
/PREP7
*SET, NU, 0.49999999
*SET, MAXIT, MAXIT+1
TB,USER,1, 1, 3
TBDATA,1, E, NU, SIGY       ! E, posn, sigy
TB,STAT,1,1,2,
TBTEMP,0
TBDATA,,E
*DIM, LBLMM, ARRAY, MAXIT, 1, 1, , ,
*DIM, UBLMM, ARRAY, MAXIT, 1, 1, , ,
*DIM, LBECM, ARRAY, MAXIT, 1, 1, , ,
*DIM, UBECM, ARRAY, MAXIT, 1, 1, , ,
*DIM, UBD,       ARRAY, MAXIT, 1, 1, , ,
```

```
*DIM, REFA,    ARRAY, MAXIT, 1, 1, , ,
UBD(1) = 1.0
FINISH
```

Appendix III: Model Macro (Axi-Symmetric Pressure Vessel)

```
/PREP7
ET,1,PLANE182
KEYOPT,1,1,0
KEYOPT,1,3,1
KEYOPT,1,6,1
*SET, RZ, 3000/1000
*SET, RB, 4500/1000
*SET, L, 3000/1000
*SET, CL, 658.2/1000
*SET, S, 225/1000
*SET, RK, 360/1000
*AFUN,DEG
K, 1,RZ,0,0,
K, 2,RZ,L,0,
K, 3,RZ-RK,L,0,
K, 4,KX(3)+RK*COS(60),KY(3)+RK*SIN(60),0,
LARC,4,2,3,RK,
K, 5,KX(4)-CL*COS(30),KY(4)+CL*SIN(30),0,
K, 6,0,KY(5)-RB*COS(30),0,
K, 7,0,KY(6)+RB,0,
LARC,7,5,6,RB,
LSTR,          4,          5
LSTR,          1,          2
K, 101,RZ+S,0,0,
K, 102,RZ+S,L,0,
K, 104,KX(3)+(RK+S)*COS(60),KY(3)+(RK+S)*SIN(60),0,
LARC,104,102,3,RK+S,
K, 105,KX(104)-CL*COS(30),KY(104)+CL*SIN(30),0,
K, 107,0,KY(6)+RB+S,0,
LARC,107,105,6,RB+S,
LSTR,          7,        107
LSTR,        105,        104
LSTR,        102,        101
LSTR,        101,          1
ALLSEL,BELOW,LINE
KSEL,INVE
KDELE,ALL
ALLSEL,ALL
NUMCMP,ALL
A, 5, 10, 9, 4
A, 4, 9, 8, 3
A, 3, 8, 7, 2
A, 2, 7, 6, 1
LSEL, S, , , 1, 4, 1,
SFL,ALL,PRES,SIGY,
LSEL,S,LOC,X,0
DL,ALL, ,UX,
LSEL,S,LOC,Y,0
DL,ALL, ,UY,
```

```
ALLSEL,ALL
LSEL,S,LENGTH,,0,S
LESIZE,ALL, , ,4, , , , ,1
CM,THICK,LINE
LSEL,S,RADIUS,,RK,RK+S
LESIZE,ALL,S/5, , , , , , ,1
CMSEL,A,THICK
LSEL,INVE
LESIZE,ALL,S/3, , , , , , ,1
ALLSEL,ALL
MSHAPE,0,2D
MSHKEY,1
AMESH,ALL
Appendix D: Post-Processing Macro
/SOL
ALLSEL,ALL
TIME,1
AUTOTS,1
NSUBST,1,0,0
ERESX,NO
OUTRES,SVAR,ALL,
*DO,LMM,1,2
*DO,K,2,MAXIT,1
/SOLU
PARSAV,ALL,'PARAM',' ',' '
*IF, K-2, GT, 0, THEN
PARRES,NEW,'PARAM',' ',' '
*ENDIF
SOLVE
/POST1
SET,LAST
UBD(K) = PL/EX*UBD(K-1)
*IF,LMM,EQ,1,THEN
LBLMM(K-1) = LBL*UBD(K-1)
UBLMM(K-1) = UBD(K)
REFA(K-1)=REF
*ELSE
LBECM(K-1) = LBL*UBD(K-1)
UBECM(K-1) = UBD(K)
*ENDIF
FINISH
*ENDDO
/SOLU
FINISH
*ENDDO
/POST26
NSOL,2,1,U,Y, Upper-LMM
NSOL,3,2,U,Y, Lower-ECM
NSOL,4,3,U,Y, Upper-ECM
NSOL,5,4,U,Y, Lower-LMM
NSOL,6,5,U,Y, Reference
STORE,MERGE
VPUT,UBLMM,2, ,
VPUT,LBECM,3, ,
VPUT,UBECM,4, ,
```

```
VPUT,LBLMM,5, ,
VPUT,REFA,6, ,
XVAR,1
/XRANGE,0,MAXIT-1
/AXLAB,Y,Limit load factor
/AXLAB,X,Iteration number
*IF,REF,LE,0,THEN
PLVAR,2,3
*ELSE
PLVAR,2,3,6
*ENDIF
```

References

[1] D. Weichert, A. Ponter, Limit States of Materials and Structures, Springer, Wien/New York, 2009.

[2] J. W. Simon, D. Weichert, Numerical lower bound shakedown analysis of engineering structures. Comput. Methods. Appl. Mech. Engrg. 200(2011) 2828–2839.

[3] A. R. S. Ponter, K. F. Carter, Limit state solutions, based upon linear elastic solutions with a spatially varying elastic modulus. Comput. Methods. Appl. Mech. Engrg. 140(1997) 237-258.

[4] A. R. S. Ponter, P. Fuschi, M. Engelhardt, Limit analysis for a general class of yield conditions. Eur. J. Mech. A/Solids, 19 (2000) 401-422.

[5] H. F. Chen, A. R. S. Ponter, Shakedown and limit analyses for 3D structures using the linear matching method. Int. J. Pre. Ves. & Piping, 78(2001) 443-451.

[6] H. F. Chen, Lower and upper bound shakedown analysis of structures with temperature-dependent yield stress. J. Pre. Ves. Tech. 132 (2010) 1-8.

[7] H. F. Chen, Linear Matching Method for Design Limits in Plasticity. Comp. Mat. & Continua, 20 (2010) 159-183.

[8] O. Barrera, A. C. F. Cocks, A. R. S. Ponter, The linear matching method applied to composite materials: a micromechanical approach. Compos. Sien. Tech. 2010.

[9] A. A. Pisano, P. Fuschi, A numerical approach for limit analysis of orthotropic composite laminates. Int. J. Num. Methods Engng. 70(2007) 71-93.

[10] A. A. Pisano, P. Fuschi, Mechanically fastened joints in composite laminates: evaluation of load bearing capacity. Composites, Part B, Eng 42(2011) 949–961.

[11] A. A. Pisano, P. Fuschi, D. De Domenico, Peak load prediction of multi-pin joints FRP laminates by limit analysis. Compos Struct 96(2013) 763–772.

[12] D. J. Tipping, The Linear Matching Method: A Guide to the ABAQUS User Subroutines", Report E/REP/BBGB/0017/GEN/07, British Energy Generation Ltd, 2008.

[13] F. A. Gaydon, A. W. McCrum, A theoretical investigation on the yield point loading of a square plate with a central circular hole. Int. J. Solids Structures, 2(1954), 156-169.

[14] D. J. F. Ewing, R. J. Spurr. The yield-point loads of symmetrically-notched pin loaded tensile strips. J. Mech. Phys. Solids. 22(1974) 27-36.

[15] A. G. Miller. Review of limit loading of structures containing defects. Int. J. Pres. Ves. & Piping. 32(1988) 197-327.

[16] Y. Yamamot, S. Asada, A. Okamoto. Round robin calculations of collapse loads-A torispherical pressure vessel head with a conical transition. ASME, J. Pres. Ves. Tech. 119(1997) 503-509.

[17] V. D. Khoi: Dual Limit and Shakedown Analysis of Structures, PhD Thesis, Université de Liége, Belgium, 2001.

[18] M. Staat, M. Heitzer, Limit and shakedown analysis for plastic safety of complex structures. Transactions of the 14th International Conference on Structural Mechanics in Reactor Technology (SMiRT 14), Vol. B, Lyon, France, August 17-22, 1997, B02/2.

[19] H. Peng, Y. H Liu, H. F. Chen, A numerical formulation and algorithm for limit and shakedown analysis of large-scale elastoplastic structures, Comput. Mech., 2018, https://doi.org/10.1007/s00466-018-1581-x

[20] H. Peng, Y. H Liu, Stress Compensation Method for Structural Shakedown Analysis, Key Eng. Mat., 794(2019), 169-181.

[21] H. Peng, Y. H Liu, H. F. Chen, J. Shen, Shakedown analysis of engineering structures under multiple variable mechanical and thermal loads using the stress compensation method, Int. J. Mech. Sci. 2018, https://doi.org/10.1016/j.ijmecsci.2018.03.020

[22] H. Peng, Y. H Liu, H. F. Chen, Shakedown analysis of elastic-plastic structures considering the effect of temperature on yield strength: Theory, method and applications, Euro. J. Mech./A Solids, 2018 https://doi.org/10.1016/j.euromechsol.2018.09.011

[23] N. K. Cho, H. Peng, Shakedown, ratchet, and limit analysis of 90 ° back-to-back pipe bends under cyclic in-plane opening bending and steady internal pressure, Euro. J. Mech./A Solids, 2017, https://doi.org/10.1016/j.euromechsol.2017.10.002